Nanomaterials and Energy
Volume 1 Issue NME1

Controlling nanomorphology in plastic solar cells
Carr, Chen, Elshobaki, Mahadevapuram and Chaudhary

ice | science

Pages 18–26 http://dx.doi.org/10.1680/nme.11.00010
Review Article
Received 04/10/2011 Accepted 08/11/2011
Published online 10/11/2011
Keywords: photovoltaics/solar cells/thin films

ice Institution of Civil Engineers
publishing

Controlling nanomorphology in plastic solar cells

1 **John A. Carr** MS
Doctoral Student
Department of Electrical and Computer Engineering, Iowa State University, Ames, USA

2 **Yuqing Chen** BS
Doctoral Student
Department of Electrical and Computer Engineering, Iowa State University, Ames, USA

3 **Moneim Elshobaki** MS
Doctoral Student
Department of Electrical and Computer Engineering, Iowa State University, Ames, USA

4 **Rakesh C. Mahadevapuram** MS
Doctoral Student
Department of Electrical and Computer Engineering, Iowa State University, Ames, USA

5 **Sumit Chaudhary** PhD
Assistant Professor
Department of Electrical and Computer Engineering, Iowa State University, IA 50011, USA; Department of Materials Science and Engineering, Iowa State University, Ames, USA





In the global search for clean, renewable energy sources, organic photovoltaics (OPVs) have recently been given much attention. Popular modern-day organic solar cells are made from solution-processable, carbon-based polymers (e.g. the model poly(3-hexylthiophene) that are intimately blended with fullerene derivatives (e.g. [6,6]-phenyl-C_{71}-butyric acid methyl ester) to form what is known as the dispersed bulk-heterojunction (BHJ). This BHJ architecture has produced some of the most efficient OPVs to date, with reports closing in on 10% power conversion efficiency. To push efficiencies further into double digits, many groups have identified the BHJ nanomorphology — that is, the phase separations and grain sizes within the polymer: fullerene composite — as a key aspect in need of control and improvement. As a result, many methods, including thermal annealing, slow-drying (solvent) annealing, vapor annealing, and solvent additives, have been developed and studied to promote BHJ self-organization. In this review, the authors present an overview of these methods and summarize the results they have enabled.

1. Introduction

Diminishing fossil fuel supplies, increasing energy demand and growing concern of carbon emission coupled with the need to acquire energy independence have spurred extensive research in alternative energy sources. In this global search, converting solar energy into electricity has been the target of many research groups in both industry and academia. Within the solar energy realm, organic photovoltaics (OPVs) are considered to be one of the most promising fields, owing to their low material and fabrication costs, mechanical flexibility, light weight, ease of processing and roll-to-roll production capability. Recently, OPV research has seen tremendous ascent, with efficiencies exceeding 7% in academia and 9% in industry (Chu *et al*., 2011a; Liang *et al*., 2010). However, to achieve the Shockley-Queisser theoretical limit, $\eta_{SQ} \approx 21\%$, (Kirchartz *et al*., 2009), much scope is left to explore.

The first OPV devices came in the late 1970s and comprised a single layer of semiconducting polymer sandwiched between two metal electrodes of different work functions. Although power conversion efficiencies (PCEs) were much less than 1% (Ghosh and Feng, 1978; Morel *et al*., 1978), this marked the advent of extensive research in the OPV field. One of the first major breakthroughs came in 1986, as Tang introduced the bilayer structure that used an acceptor (a perylene tetracarboxylic derivative) stacked on top of a donor (copper phthalocyanine) and touted an efficiency of about 1% (Tang, 1986). When light is incident on an OPV device, photons are absorbed in the donor polymer and Coulombically bound electron–hole pairs, called excitons, are generated. Unlike their inorganic counterparts, organic semiconductors have the disadvantage of a low relative permittivity (around 3), which causes the exciton binding energies (0·2–0·7 eV) to be more than an order of magnitude higher than the

thermal energy at room temperature. As a result, exciton diffusion must take place to an interface, where band offsets can assist with excition dissociation into free carriers. Thereafter, the electric field generated by the difference between the electrodes work-functions sweeps the free charges through the donor (holes) and acceptor (electrons) to the anode (holes) and cathode (electrons) where they can be stored or used to do electrical work on an external system. When compared to single layer OPVs, which contain dissociation interfaces only at the electrode/polymer junctions, bilayer structure (Figure 1(a)) introduces a new interface between donor and acceptor entities to dissociate more excitons and improve overall efficiency.

The bilayer structure marked an important breakthrough, but a major limitation still existed: excitons are created across the entire bulk of the organic semiconducting layer, but only those within circa 10 nm of an interface will be dissociated. Further, to absorb a large majority of incident photons, the semiconductor layer must be at least 100nm thick. Thus, a fundamental bottleneck exists: the active material must be thick for high absorbance, but thin for a high probability of exciton dissociation. To address this issue, a revolutionary development then came in the mid-1990s with the demonstration of a dispersed bulk heterojunction (BHJ) architecture (Halls *et al*., 1995; Yu *et al*., 1995). Here, the acceptor and donor materials are blended together to create an interpenetrating network with a thickness sufficient for photon absorption and a phase separation nearing the exciton diffusion length (Figure 1(b)). Since its inception, nearly all groups working with solution processable OPVs have adopted the BHJ structure and many studies have closely linked its performance to the active layer morphology – that is, the degree of horizontal and vertical phase-separation (between the donor and acceptor), as well as, the grain size and crystallinity of the composite materials. Since most as-cast BHJ systems are not completely optimized, several important limitations exist. First, it is well known that the active layer of the disordered BHJ architecture has a tendency to produce cul-de-sacs (i.e. dead-ends) in the charge transport pathways. These regions can act as sources of charge loss either in the form of recombination centers or space charge centers leading to undesirable distortions of electric field in the active layer. Secondly, some BHJ based cells (depending on materials and solvents used) have been shown to suffer from the formation of an undesirable vertical phase separation (i.e. too much donor near the cathode or too much acceptor near the anode). These regions can act as tunnel barriers, blocking charge collection at the electrode; or as shunt pathways between anode and cathode. Lastly, many reports have found the formation of too small (or too large) material domains in the BHJ structure. These regions can greatly impede charge mobilities (small grain formation) or greatly impede exciton dissociation (large grain formation). In summary, an un-optimized morphology can lead to greater recombination losses, higher series resistances and limited fill-factors in these devices (Kim *et al*., 2006). To overcome, careful manipulation of phase separation and grain formation must be used to achieve the best molecular order in the BHJ OPVs. As a result, many reports on methods to control and improve the nanomorphology of the BHJ active layer have surfaced within the last 5–10 years. Herein, we compile the OPV community's knowledge-to-date on BHJ self-organization by various processes, including post-production thermal annealing (TA), mid-production TA, slow-growth-solvent annealing, vapor annealing and solvent additives (SA).

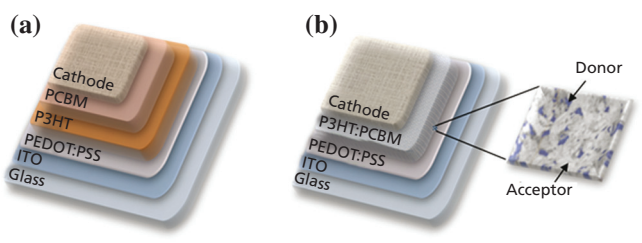

Figure 1. Schematic diagram of organic photovoltaic (a) bilayer and (b) bulk-heterojunction architectures

2. Thermal annealing

In improving OPV morphology, TA is widely employed as a primary strategy. TA is a well-known metallurgical technique that is, among other things, commonly used for the strengthening, crystallization and lattice repair of many metals and inorganic semiconductors. Much the same for organic semiconductors, a report in 1995 shows that when a polythiophene (such as P3HT) is annealed at temperatures greater than its glass-transition temperature, an enhanced crystallization is noticed (Zhao *et al*., 1995). Thus, to improve active layer crystallization, this process has been applied during BHJ OPV fabrication in both a post-production (i.e. after cathode deposition) and mid-production (i.e. immediately after spin coating) technique. Reports as early as 2000 and 2002 began utilizing TA on distributed heterojunction-based cells in an effort to improve conversion efficiencies (Camaioni *et al*., 2002; Dittmer *et al*., 2000; Schilinsky *et al*., 2002). One of the pioneering BHJ annealing reports came in 2003, when Padinger *et al*. presented a novel post-production treatment in which both heat and direct current (DC) bias were applied (Padinger *et al*., 2003). The group reports an as-cast efficiency of only 0·4% for P3HT:PCBM based BHJs at a 1:2 weight ratio. However, after a 75°C, 2·7 V treatment, efficiency improves to 3·5% – a nearly nine-fold enhancement. Interestingly, cells treated without the DC bias (i.e. TA only) increased only six-fold to 2·5%; the difference being imputed to the applied bias burning out parasitic shunt paths. The external quantum efficiency (EQE) of both treated cells showed slight red shift and definite formation of vibronic peaks (Figure 2); both of which are indicative of better crystallinity in the polymer layer. Following Padinger's work, Chirvase *et al*. further investigated post-production annealing on a P3HT:PCBM systems of varying PCBM concentrations (namely, 1:0·7, 1:0·8, 1:0·9, 1:1, 1:1·5,1:2 and 1:3) treated at 130°C for 20 seconds (Chirvase *et al*., 2004). Here, the authors reported a significant enhancement in

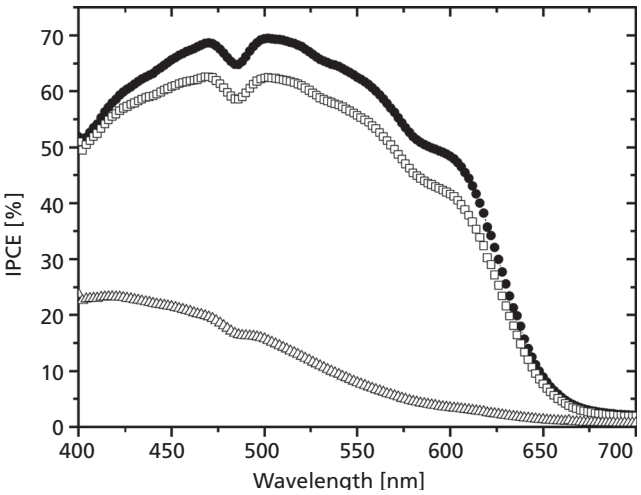

Figure 2. External quantum efficiency (EQE) of P3HT-PCBM solar cells: as-produced solar cell [open triangles], annealed solar cell [open squares], and cell simultaneously treated by annealing and applying an external voltage [filled circles]. Reprinted with permission from (Padinger *et al*., 2003). Copyright [2003], Wiley

short circuit current and EQE upon thermal treatment, regardless of PCBM loading. Also in 2004, Hoppe *et al*. included annealing effects in their modeling of optical absorption in conjugated BHJ cells (Hoppe *et al*., 2004). Here, from optical considerations, the authors predicted currents of 6·34 mA/cm^2 (as-cast), 8·42 mA/cm^2 (thermally annealed) and 9·02 mA/cm^2 (thermally annealed and biased). Comparing theses numbers to the EQE of Pradinger's 2003 work, Hoppe asserted optical effects alone may account for upto 40% of the improved device efficiency.

In 2005, Savenije *et al*. then applied mid-production TA to P3HT:PCBM BHJ based cells and studied its influence on the morphological and photoconductive device properties. After annealing at 80°C, the active layer was shown to form more crystalline fibrils of P3HT (Figure 3). These fibrils are the result of a higher order packing of the polymer chains, resulting in a homogeneous distribution of P3HT crystals (Savenije *et al*., 2005). Further, the increased packing was shown to lead to higher charge mobility, with hole mobility increasing from 0·0056 cm^2 V^{-1}s^{-1} to 0·044cm^2 V^{-1}s^{-1}after TA. It is interesting to note that the authors quote 'extreme phase separation' at higher annealing temperatures (circa 130°C), with crystals reaching the micrometer regime. Also in 2005, Kim *et al*. extended TA studies and included a comparison of both annealing temperature (25–225°C, increments of 25°C) and solvent choice (chlorobenzene (CB) and di-cholorbenzene (DCB)) on a P3HT:PCBM 1:1 BHJ system (Kim *et al*., 2005). Devices cast from CB and annealed at 140°C (circa 30°C above P3HT glass-transition) produced the most efficient cells (circa 3%) in this study. In a similar study, Reyes-Reyes *et al*. study the effects of TA on what the authors call an optimally loaded P3HT:PCBM system – that is, P3HT:PCBM in a 1:0·8 weight ratio (Reyes-Reyes

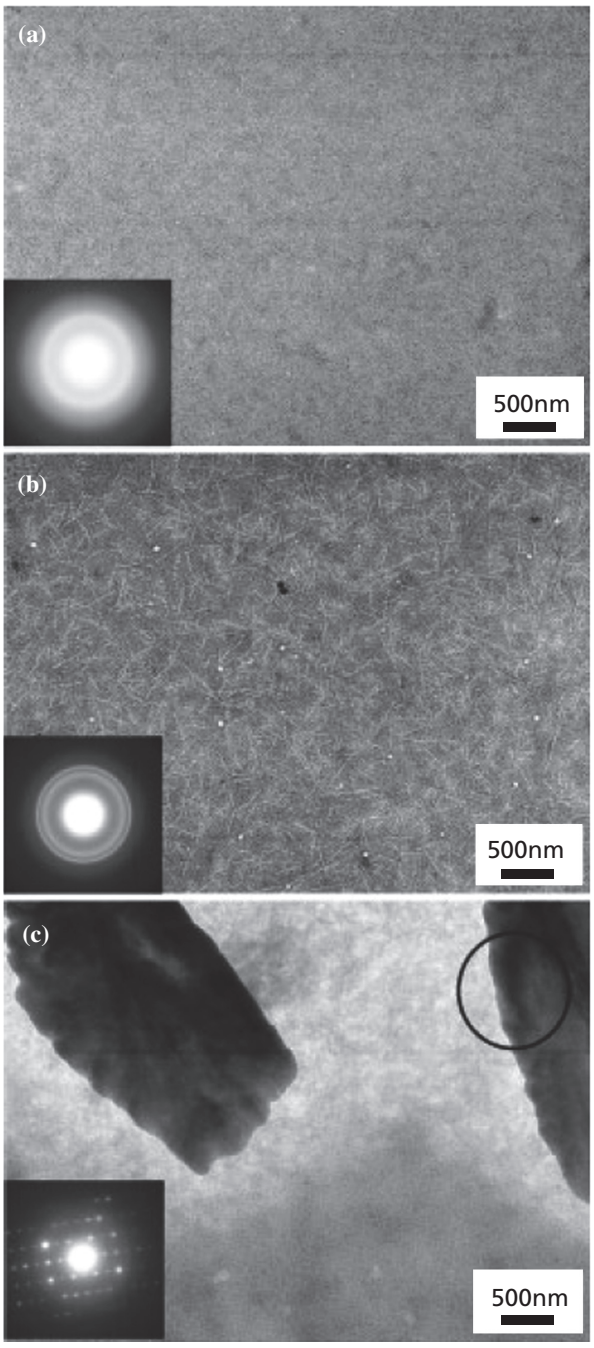

Figure 3. Bright-field (BF) TEM images of 1:1 PCBM:P3HT composite film in pristine condition (a), after thermal annealing at 80°C (b), and after thermal annealing at 130°C (c). The inserts are the corresponding selected-area electron diffraction (SAED) patterns. Reprinted with permission from (Savenije *et al.*, 2005). Copyright [2005], Wiley

et al., 2005). A short annealing treatment of 155°C, in conjunction with optimal PCBM weight, produced cells nearing 5·0% efficiency. Next, Erb *et al*. gave an in-depth study relating TA to active layer

crystallinity, confirming earlier reports and adding much detail (Erb *et al*., 2005). The group reported that the annealing of P3HT:PCBM thin films leads to the formation of P3HT crystallites, such that, P3HT main chains orient parallel, and their side chains perpendicular, to the substrate.

Again in 2005, while attempting to optimize a 1:1 weight ratio P3HT:PCBM based system, Li *et al*. found the TA conditions to be of upmost importance to device efficiency (Li *et al*., 2005b). After optimization, the group demonstrated a 4·0% efficient device. Ultraviolet-visible absorption spectroscopy (UV-vis) and atomic force microscopy (AFM) were used to explain the effect of TA. The UV-vis absorption spectra showed a redshift after post-production annealing at temperatures spanning from 70 to 100°C with times from 4 to 40 minutes. This shift was imputed to an increased interchain interaction among P3HT chains, which results in more delocalized conjugated π electrons. This delocalization lowers the band gap between π and π*, which leads to the observed red shift. Analogously, this is to say a more crystalline film is formed after annealing, again supporting Pandinger's and Savenije's original reports. AFM images show the active layer surface becoming rougher while increasing the TA temperature from 70 to 110°C, then less rough for temperatures from 110 to 150°C. Further, PCEs followed a similar trend with 110°C producing the best devices and 150°C producing the worst (aside from as-cast). From this, the authors assert an interesting relation between performance and morphology – higher roughness films lead to higher OPV efficiencies. Following this work, Ma *et al*. achieve PCEs again approaching 5% with the model P3HT:PCBM based BHJ architecture (Ma *et al*., 2005). The authors fully attribute their enhanced performance to changes induced by a 150°C, post-production heat treatment.

In 2006, Mihailetchi *et al*. further investigated the effects of TA on charge carrier mobility (Mihailetchi *et al*., 2006). Here, P3HT:PCBM (1:1 by weight) based BHJ devices were post-production annealed for 4 minutes at both 70 and 120°C. This report found improved mobility to be the most important aspect leading to efficiency enhancements. Hole mobility was discerned to have a more significant annealing enhancement (circa 10^{-11} m^2 $V^{-1}s^{-1}$ to 10^{-8} m^2 $V^{-1}s^{-1}$) than the electron mobility (circa 10^{-8} to 10^{-7} m^2 $V^{-1}s^{-1}$), indicating that the stacking of P3HT domains is affected more greatly than that of the PCBM domains. Another study in 2006 systematically analyzes studies different P3HT:PCBM blend ratios in conjunction with various TA conditions (Swinnen and Haeldermans, 2006). Here, the authors report a dependence of crystallization kinetics on temperature/duration. At short (<5min), low (75–100°C) TA conditions, P3HT crystallizes; while at increasing times and temperatures, needle-like PCBM aggregates (up to 100 μm in size) form.

In the following year, a work by Nguyen *et al*. presented a comparative study on the effects involved in the annealing process on poly-(3-alkylthiophene)s (P3ATs) of differing side-chain lengths (Nguyen *et al*., 2007). The authors found that, for each P3AT:PCBM blend, annealing parameters (i.e. temperature and time) need to specifically optimized. For example, P3DT performed best with a 75°C, 5 minutes treatment, while P3BT preferred 160°C for 30 seconds. Further, the group proposes two main morphological changes during TA: (i) the enhancement of polymer crystallization (leading to improved absorption and hole mobility) and (ii) the diffusion of PCBM (leading to an increased phase separation); supporting Swinnen and Haeldermans's observation in 2006. In 2008, Clarke *et al*. further investigated the origin of TA induced short circuit current (J_{sc}) enhancement in P3HT:PCBM BHJ cells (Clarke *et al*., 2008). Using transient absorption spectroscopy, the authors show a nearly two-fold increase in dissociated charges within the blend. The increase is attributed to a circa 50 meV reduction of the ionization potential resulting from the crystallization of P3HT during heat treatment. Consequently, three main enhancement channels had been identified to-date: optical effects (Hoppe *et al*., 2004), hole transport (Mihailetchi *et al*., 2006) and exciton dissociation (Clarke *et al*., 2008).

More recently Wang *et al*. continued work on the investigation of BHJ TA (Wang *et al*., 2011). Here, four distinct, advantageous TA-induced processes were identified: (i) the evaporation of residual solvent at temperatures above the glass transition of the blend, (ii) the relaxation of non-equilibrium molecular conformation, (iii) the crystallization of both P3HT and PCBM components and (iv) the phase separation of P3HT and PCBM domains. One notices (iii) and (iv) are in agreement with Nguyen's 2007 proposal. In addition, this study found that the rate at which the active layer is returned to room temperature is an important consideration of the isothermal annealing process. Linear cooling rates between 8 and 90°C $minutes^{-1}$ produced better PCEs than immediate cooling (i.e. transferring the substrate from a hot stage to a cold steel plate). The rapid quenching of active layer heat is expected to inhibit the crystallization of the polymer and can trap non-equilibrium morphological states, thereby reducing OPV performance.

3. Slow-growth-solvent and vapor annealing

Aside from TA, a second, heatless annealing process was first applied to BHJ OPVs (Li *et al*., 2005a). This process, now known as *slow drying* or *solvent annealing* and referred to here as *slow-growth-solvent annealing*, involves storing the active layer film in a confined volume (such as a glass petridish) directly after spin-coating to allow the solvent to dry more slowly. In their important 2005 work, Li *et al*. studied the difference between fast grown (i.e. as-cast films) and slow grown (i.e. films slow dried under a glass dish) films and reported a PCE of 4·4% – one of the highest published at the time. In 2006, the same group further investigated the fast against slow grown devices to showed significant generation, dissociation and mobility improvements (Shrotriya *et al*., 2006). One notices, these enhancements are similar to those identified for the TA process. Here, hole mobility was shown to increase from

~1·9 × 10^{-9} to ~1·7 × 10^{-7} m^2 $V^{-1}s^{-1}$ and electron mobility from ~6·5 × 10^{-8} to ~2·6 × 10^{-7} m^2 $V^{-1}s^{-1}$ (a more balanced charge transport in slow grown case can also be noted). Further, photocurrent characterization showed an increased generation rate in slow grown films and, by applying the Braun modified Onsager model, the authors were able to suggest a 47–51% dissociation rate for fast grown films compared to a 70–80% rate for slow gown (Figure 4). Work on solvent annealing was again continued by Yang Yang's group in 2007 (Li *et al*., 2007). In this work, a systematic study of solvent annealing as a function spin speed (t_s) was presented. The solvent annealing time (t_a), which is the time taken by the solvent to dry after spin coating, was monitored and correlated to both t_s and device performance. Using photophysical and morphological characterization techniques, the authors were able to reveal an optimal t_a (>60 s; corresponding to t_s > 50 s) for greatest devices performance and show solvent annealing is most powerful at higher PCBM loadings. Again in 2008, Miller *et al*. published on the effects of similar morphological control technique, vapor annealing – that is, the exposure of OPV BHJ devices to solvent fumes (which can be different from the host solvent) after the film has dried (Miller *et al*., 2008). In their study, P3HT was shown to increase in ordering, improving crystallinity and providing better charge transport. The authors asserted that vapor annealing is comparable in performance to both thermal and solvent annealing, but advantageous owing to its lack of heat (compared to TA) and speed (1 minutes length compared to the 20 minutes+ increase in dry times of slow-growth-solvent annealing).

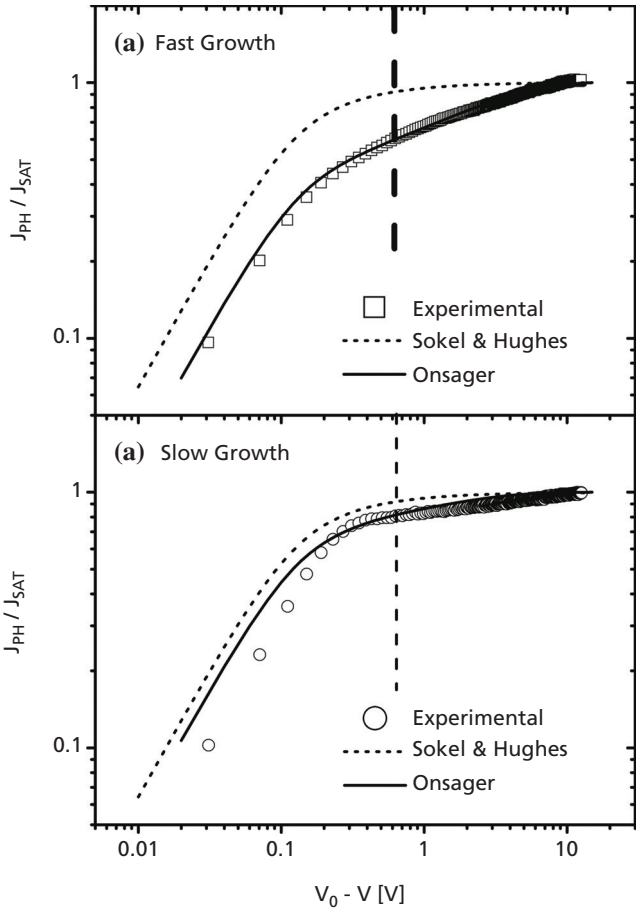

Figure 4. Measured (open symbols) and calculated (solid curves) normalized photocurrent as a function of effective applied bias for (a) fast and (b) slow grown films. The solid curves represent the J_{ph}/J_{sat} values calculated from Onsager's model. Reprinted with permission from (Shrotriya *et al*, 2006). Copyright [2006], American institute of Physics

In 2009, research employing vapor annealing continues with Bull *et al*.'s work on mesocopic PCBM crystallites (Bull *et al*., 2009). Here, poly(5,7-bis(3-dodecylthiophene2-yl) theino[3,4-b] pyrazine-alt-9,9-dioctyl2,7-flourene) (BTTP-F):PCBM cells were treated post-production by way of degassed CB. The group found the expected performance improvement, however; showed an unfavorable change in vertical film morphology, as well as, the formation of very large PCBM crystallites, similar to the observation of Swinnen and Haeldermans in 2006. Thus, the authors suggest that the inclusion of new methods for nucleating the desired nanomorphology, without having to include such large PCBM aggregates, could induce further performance enhancements.

A pinnacle 2008 work by Campoy-Quiles *et al*. compares the above-mentioned nanomorphology control techniques (fast drying, slow-growth-solvent annealing, TA and vapor annealing) to better understand the molecular rearrangement and kinetics of the morphological changes (Campoy-Quiles *et al*., 2008). Here, the authors remind that the various techniques produce similar results, with PCEs ranging from 4 to 5%. Further, it is shown that all techniques lead to a common arrangement of the composite blend, where P3HT initially crystallizes, encouraging the diffusion of PCBM to nucleation sites – where PCBM aggregates can grow.

4. Solvent additives

In addition to the above-mentioned annealing methods, solvent additives (SAs) have also been explored as a viable alternative for intelligent control of OPV morphology. When compared to annealing techniques, it has been asserted that SAs are a fundamentally better option. This claim was made on the basis of a single reason: the phases separate during spin-casing, in a single processing step. This makes for easier, quicker fabrication without the need for heat treatment or lengthening drying times. Research on SAs has been ongoing for more than five years and, thus far, has produced exceptional results; with at least one account of PCEs tripling upon the addition of SA.

The first reports on SAs surfaced in 2006 (Peet *et al*., 2006; Zhang *et al*., 2006). A work by Zhang *et al*. shows solvent mixing was advantageous to the morphology of polyflourene copolymer/fullerene

blended OPVs and thereby, were able to enhance their PCE by 0·2 percentage points (Zhang *et al*., 2006). Just months later, a work by Peet *et al*. (2006) showed that mixing a small-volume additive (e.g. octylthiol) into a host solvent (e.g. toluene) decreased the optical transmittance of P3HT:PC_{61}BM OPVs, red shifted the spectra, and gave rise to more distinct vibronic peaks (Figure 5).These observations, of course, are in line with the earlier works on thermal, slow-growth-solvent and vapor annealing. The authors showed these changes as a result of an enhancement in P3HT crystallinity and, further, were able to quantify an increase in carrier lifetime which is indicative of a reduction in mid-gap defect states. In this same work, Peet el al. offered the first insights into SA selection, indicating that enhancement was independent of solvent boiling point or polarity.

Since the original reports, many works have explored these processing additives. In 2007, Peet *et al*. again published positive SA results. Here, the authors incidentally discovered that the incorporation of small concentrations of alkanethiols modified P3HT:PCBM nanoscale morphology. Further, while working with a low-band gap polymer, poly[2,6-(4,4-bis-(2-ethylhexyl)-4H-cyclopenta [2,1-b;3,4-b']-dithiophen)-*alt*-4,7-(2,1,3-benzothiadiazole)] (PCPDTBT), Peet *et al*. found that TA techniques were ineffective at controlling PCPTBT/PCBM phase separation. Thus, the group applied the alkanethiols finding and was able to improve PCE from 2·8 to 5·5%. In the same year, Lee *et al*. attempted to further characterize and explain the alkanedithiols-induce efficiency enhancement (Lee *et al*., 2008). Based on alkanedithiol's high boiling point (higher than the host cholorobenzene solvent) and its selective solubility of PCBM, the authors predicted three different phases during the crystallization kinetics of the composite film: (*i*) a fullerence–alkanedithiol phase, (*ii*) a polymer aggregate phase and (*iii*) a polymer–fullerene phase (Lee *et al*., 2008). Considering these phases, one can readily see how larger polymer and fullerene crystals are encouraged. During spin-casting/drying, the lower boiling point host solvent rapidly evaporates causing the materials to condense into domains and form a film. The higher boiling point additive evaporates more slowly, allowing phase (i) to remain as a solution longer. This causes both PCBM and P3HT to cluster and form larger, more crystalline domains. AFM confirmed different additives give different domain sizes and shapes (Figure 6). From their phase theory, Lee *et al*. offered two criteria for the selection of practical additives: (*i*) the SA should have a lower vapor pressure (i.e. higher boiling point) than the host solvent and (*ii*) the SA should have selective solubility of one of the materials (e.g. PCBM) (Lee *et al*., 2008). In 2008, Yao

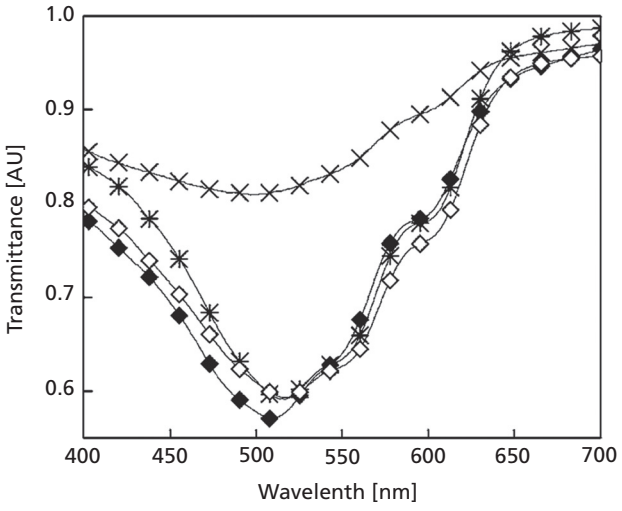

Figure 5. Transmittance through films for films on glass substrates: neat solvent/no annealing (X), neat solvent/150°C 15 min annealing (*), 1% *n*-octylthiol/no annealing (♦), and 1% *n*-octylthiol/ 150°C 15 min annealing (◊). Reprinted with permission from (Peet *et al.* 2006). Copyright [2006], American institute of Physics

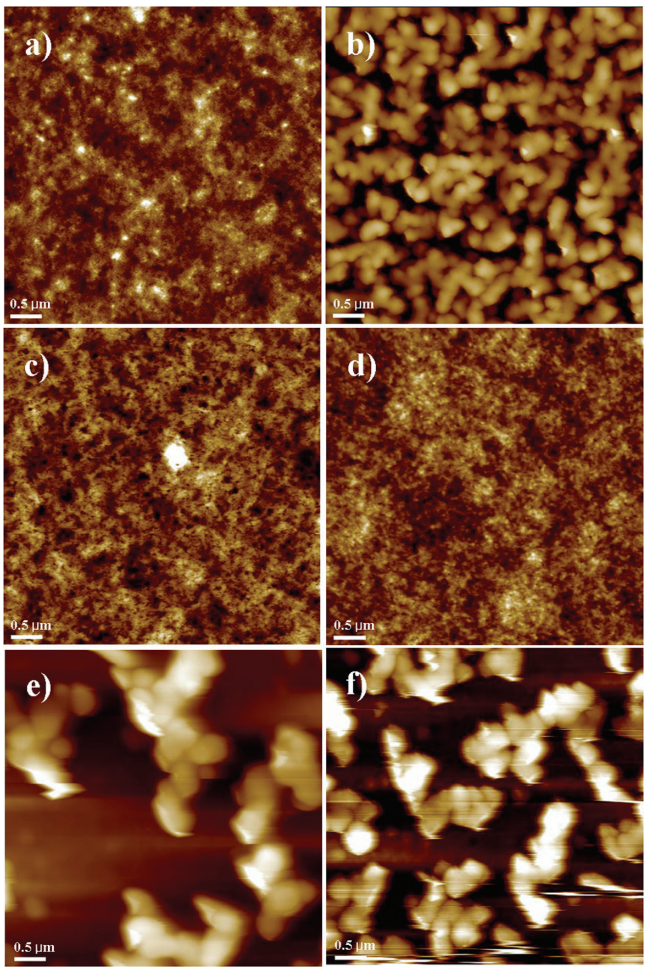

Figure 6. AFM topography of films cast from PCPCTBT/C71-PCBM with additives: (a) 1,8-octanedithiol, (b) 1,8-cicholorooctane, (c) 1,8-dibromooctane,(d) 1,8-diiodooctane, (e) 1,8-dicyanooctane and (f) 1,8-octanediacetate. Reprinted with permission from (Lee *et al.*, 2008). Copyright [2008] American Chemical Society

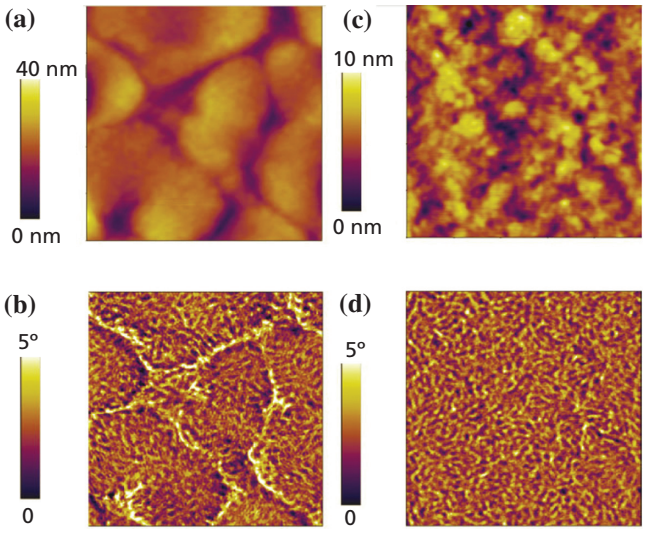

Figure 7. Topography (a, c) and phase (b, d) images of ITO/PEDOT:PSS/poly[(4,4-didodecyldithieno[3,2-*b*:2′,3′-*d*]-2,6-diyl-*alt*-(2,1,3-benzoxadiazole)-4,7-diyl]:$PC_{71}BM$ films made without using CN (a, b) and with CN (c, d). The scan size of the images is 1 × 1 μm.Reprinted with permission from (Hoven *et al.*, 2010). Copyright [2010], Wiley

et al. corroborated these criteria and offered a third addition: (*iii*) the additive must be miscible with the host solvent (Yao *et al*., 2008). In their work, Yao *et al*. first explored a 1,8-octanedithiol (OT) additive to the model P3HT:PCBM system (1,2-dichlorobenzene (*o*-DCB) host solvent) and then extended their results to include two new additives di(ethylene glycol)-diethyl ether and *N*-methyl-2-pyrrolidone. The authors were able to produce varying efficiency enhancements with all three additives, allowing them to suggest the chemical properties of the additive are irreverent, while the physical properties remain most important. Most interestingly, in contrast to the original observation that enhancement is independent of additive boiling point, it was emphasized that the boiling point of the SA should not be too high to ensure all (or more practically, most) solvent is removed upon drying.

In 2010, SA exploration was continued by Hoven *et al*. (2010). In this work, a novel donor polymer, poly[(4,4-didodecyldithieno [3,2-*b*:2′,3′-*d*]-2,6-diyl-*alt*-(2,1,3-benzoxadiazole)-4,7-diyl] was introduced with a PCE of circa 1·6%. After the introduction of 1-chloronaphthalene (CN) as a small-volume additive (cholorobenzene host solvent), PCEs more than tripled to circa 4·9%. Most notably, Hoven *et al*. showed a significant *reduction* in surface roughness and a *reduction* in phase domain size upon the addition of CN (Figure 7). Interestingly, this is in contrast to a majority of other reports, in which, additives give rougher films with larger domains. Further, this is in contrast to Li *et al*.'s theory that rougher films give better performing devices. However, it should be considered that Hoven *et al*. have gone against criterion (ii) and used an additive in which both polymer and fullerene are soluble. Further, both materials have a better solubility in the CN additive as compared with the host CB (Hoven *et al*., 2010). Therefore, whereas most use a *better* host solvent and add a *poorer* and/or selective small-volume solvent, Hoven *et al*. use a *poorer* host with a *better*, non-selective additive. Thus, this opposite result could be expected. Nonetheless, Hoven's work highlights the versatility of small-volume SAs, indicating that not only can aggregation be encouraged during crystallization kinetics, but it can also be discouraged. After Hoven's report, Salim *et al*. investigated deeper into the effects of SAs on the model P3HT:$PC_{61}BM$ blend (Salim *et al*., 2010). Here, the authors directly compared the effect of additive boiling point and solubility on nanoscale phase separation. Alkanedithiols with similar chemical structure but differing boiling points and solubility were incorporated with the host *o*-DCB. Salim *et al*. found that improvement is not linear with increasing boiling point, but resembles a bell shape. This corroborates earlier reports which have predicted that boiling points should be high (Lee *et al*., 2008), but not too high (Yao *et al*., 2008). Of the four SAs explored, the authors found the middle two (namely, 1,6-hexanedithiol with t_b = 242°C and 1,8-octanedithiol with t_b = 270°C) perform better than the outer two (namely 1,5-pentanedithiol with t_b = 216°C and 1,9-nananedithiol with t_b = 294°C). Further, the authors were able to show that there is an optimal combination between boiling point and solubility for the best performing SA. This work further supports the 2008 publication by Yao *et al*., in which, they suggest additive chemical properties are irrelevant compared to additive physical properties.

More recently, Chang *et al*. increments SA work in 2011 exhibiting the effect of trace solvent on the nanomorphology of P3HT:PCBM BHJ solar cells (Chang *et al*., 2011). In this report, gas chromatography–mass spectrometry was used to show entrapped solvent within the BHJ film, despite a 10 minutes, 150°C heat treatment. As a result, the group found larger PCBM agglomerates and a more extensive phase separation. Interestingly, an *o*-DCB host solvent resulted in larger domains than a CB host solvent. To combat this, the authors added a small volume fraction of nitrobenzene (NB) to the host solution, which prevented PCBM diffusion and, thereby, aggregation (Figure 8). Those devices cast with NB performed similarly to thermally annealed, CB-cast cells and were shown be less affected by prolonged heat treatment (i.e. more thermally stable). Most importantly to note, NB is a non-solvent for both P3HT and PCBM and, thus, Chang has shown criterion (ii) (as mentioned above) should be reconsidered. A second work on SAs in 2011 came from Chu *et al*. Here, the authors present results on two new additives, dimethylsulfoxide (DMSO) and dimethyl formamide (DMF), to a poly[*N*-heptadecanyl-,7-carbazole-*alt*-5,5-(4′,7′-di-2thienyl-2′,1′,3′-benzothiadiazole)] (PCDTBT):$PC_{71}BM$ system (*o*-DCB host solvent) (Chu *et al*., 2011b). Using 10–13% by volume of SA, the authors were able increase PCE by as much as 18%. In alignment with earlier reports, the authors showed the additives significantly increase surface roughness, domain size and hole mobility. More interestingly, neither DMSO nor DMF dissolve either material (PCDTBT nor $PC_{71}BM$) and DMF has a lower boiling

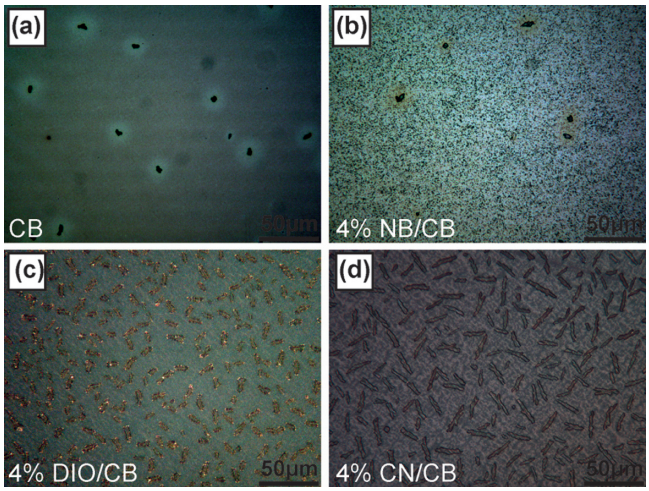

Figure 8. Microscope images of P3HT/PCBM (1:1) films spin-coated from (a) CB, (b) 4% NB added to CB, (c) 4% DIO added to CB and (d) 4% CN added to CB. Films were heat-treated in a glove box for 30 min at 150°C.Reprinted with permission from (Chang *et al*., 2011). Copyright [2011], Wiley

point than the host *o*-DCB (Chu *et al*., 2011b). Consequently, the authors have again strayed from the above-mentioned SA selection criteria and, along with Chang *et al*., have opened the door for future exploration of non-selective, low-boiling point additives.

5. Conclusions

In summary, several types of treatments have been used to optimize the nanomorphology of donor–acceptor blend films in OPVs, and to improve PCE of resultant devices. Several models and reasons have been proposed for the observed improvements, and there are ample agreements as well as contradictions among different groups and experiments. Knowledge discovery in this direction is still evolving, and so is the choice of annealing treatments with the emergence of solar cells based on new organic semiconductors. What works for one material, does not always work for another due to differences in chemical structures and type of molecular packing in thin films. Thus, as the field of organic solar cells advances, more progress is expected on the front of controlling and understanding nanomorphology, as well as elucidation of process-structure-property interrelationships.

REFERENCES

Bull TA, Pingree LSC, Jenekhe SA, Ginger DS and Luscombe CK (2009) The role of mesoscopic PCBM crystallites in solvent vapor annealed copolymer solar cells. *ACS nano* **3**: 627–636.

Camaioni N, Ridolfi G, Casalbore MG, Possamai G and Maggini M (2002) The effect of a mild thermal treatment on the performance of poly(3 alkylthiophene)/fullerene solar cells. *Advanced Materials* **14**: 1735–1738.

Campoy-Quiles M, Ferenczi T, Agostinelli T *et al*. (2008) Morphology evolution via self-organization and lateral and vertical diffusion in polymer:fullerene solar cell blends. *Nature Materials* **7**: 158–164.

Chang L, Lademann HWA, Bonekamp J.-B, Meerholz K and Moulé AJ (2011) Effect of trace solvent on the morphology of P3HT:PCBM bulk heterojunction solar cells. *Advanced Functional Materials* **21**: 1779–1787.

Chirvase D, Parisi J, Hummelen JC and Dyakonov V 2004 Influence of nanomorphology on the photovoltaic action of polymer–fullerene composites. *Nanotechnology* **15**: 1317–1323.

Chu T-Y, Lu J, Beaupré S *et al*. (2011a) Bulk heterojunction solar cells using thieno[3,4-c]pyrrole-4,6-dione and dithieno[3,2-b:2',3'-d]silole copolymer with a power conversion efficiency of 7·3%. *Journal of the American Chemical Society* **133**: 4250–4253.

Chu T-Y, Lu J, Beaupré S *et al*. (2011b) Morphology control in polycarbazole based bulk heterojunction solar cells and its impact on device performance. *Applied Physics Letters* **98**: 253301 (1–3).

Clarke TM, Ballantyne AM, Nelson J, Bradley DDC and Durrant JR (2008) Free energy control of charge photogeneration in polythiophene/fullerene solar cells: The influence of thermal annealing on P3HT/PCBM Blends. *Advanced Functional Materials* **18**: 4029–4035.

Dittmer JJ, Marseglia EA and Friend RH (2000) Electron trapping in dye/polymer blend photovoltaic cells. *Advanced Materials* **12**: 1270–1274.

Erb T, Zhokhavets U, Gobsch G *et al*. (2005) Correlation between structural and optical properties of composite polymer/fullerene films for organic solar cells. *Advanced Functional Materials* **15**: 1193–1196.

Ghosh AK and Feng T (1978) Merocyanine organic solar cells. *Journal of Applied Physics* **49**: 5982-5989.

Halls JJM, Walsh CA, Greenham NC *et al*. (1995) Efficient photodiodes from interpenetrating polymer networks. *Nature* **376**: 498–500.

Hoppe H, Arnold N, Meissner D and Sariciftci N (2004) Modeling of optical absorption in conjugated polymer/fullerene bulk-heterojunction plastic solar cells. *Thin Solid Films* **451**: 589–592.

Hoven CV, Dang XD, Coffin RC *et al*. (2010) Improved performance of polymer bulk heterojunction solar cells through the reduction of phase separation via solvent additives. *Advanced Materials* **22**: E63–E66.

Kim JY, Kim SH, Lee HH *et al*. (2006) New architecture for high-efficiency polymer photovoltaic cells using solution-based titanium oxide as an optical spacer. *Advanced Materials* **18**: 572–576.

Kim Y, Choulis SA, Nelson J *et al*. (2005) Device annealing effect in organic solar cells with blends of regioregular poly (3-hexylthiophene) and soluble fullerene. *Applied Physics Letters* **86**: 063502–063503.

Kirchartz T, Taretto K and Rau U (2009) Efficiency limits of organic bulk heterojunction solar cells. *Journal of Physical Chemistry C* **113**: 17958–17966.

Lee JK, Ma WL, Brabec CJ *et al*. (2008) Processing additives for improved efficiency from bulk heterojunction solar cells. *Journal of the American Chemical Society* **130**: 3619–3623.

Li G, Shrotriya V, Huang JS *et al*. (2005a) High-efficiency solution processable polymer photovoltaic cells by self-organization of polymer blends. *Nature Materials* **4**: 864–868.

Li, G., Shrotriya V, Yao Y and Yang Y (2005b) Investigation of annealing effects and film thickness dependence of polymer solar cells based on poly(3-hexylthiophene). *Journal of Applied Physics* **98**.

Li G, Yao Y, Yang H *et al*. (2007) "Solvent annealing" effect in polymer solar cells based on poly(3-hexylthiophene) and methanofullerenes. *Advanced Functional Materials* **17**: 1636–1644.

Liang Y, Xu Z, Xia J *et al*. (2010) For the bright future — bulk heterojunction polymer solar cells with power conversion efficiency of 7.4%. *Advanced Materials* **22**: E135–E138.

Ma WL, Yang CY, Gong X, Lee K and Heeger AJ (2005) Thermally stable, efficient polymer solar cells with nanoscale control of the interpenetrating network morphology. *Advanced Functional Materials* **15**: 1617–1622.

Mihailetchi VD, Xie HX, De Boer B, Koster LJA and Blom PWM (2006) Charge transport and photocurrent generation in poly(3-hexylthiophene): methanofullerene bulk-heterojunction solar cells. *Advanced Functional Materials* **16**: 699–708.

Miller S, Fanchini G, Lin YY *et al*. (2008) Investigation of nanoscale morphological changes in organic photovoltaics during solvent vapor annealing. *Journal of Materials Chemistry* **18**: 306–312.

Morel DL, Ghosh AK, Feng T *et al*. (1978) High-efficiency organic solar cells, AIP.

Nguyen L, Hoppe H, Erb T *et al*. (2007) Effects of annealing on the nanomorphology and performance of poly (alkylthiophene): fullerene bulk heterojunction solar cells. *Advanced Functional Materials* **17**: 1071–1078.

Padinger F, Rittberger RS and Sariciftci NS (2003) Effects of postproduction treatment on plastic solar cells. *Advanced Functional Materials* **13**: 85–88.

Peet J, Soci C, Coffin R *et al.* (2006) Method for increasing the photoconductive response in conjugated polymer/fullerene composites. *Applied Physics Letters* **89**: 252105–252105-3.

Peet J, Kim JY, Coates NE *et al*. (2007). Efficiency enhancement in low-bandgap polymer solar cells by processing with alkane dithiols. *Nature Materials* **6**: 497–500.

Reyes-Reyes M, Kim K and Carroll DL (2005) High-efficiency photovoltaic devices based on annealed poly (3-hexylthiophene) and 1-(3-methoxycarbonyl)-propyl-1-phenyl-(6, 6) C blends. *Applied Physics Letters* **87**: 083506.

Salim T, Wong LH, Bräuer B *et al*. (2010) Solvent additives and their effects on blend morphologies of bulk heterojunctions. *Journal of Materials Chemistry* **21**: 242–250.

Savenije TJ, Kroeze JE, Yang X and Loos J (2005) The effect of thermal treatment on the morphology and charge carrier dynamics in a polythiophene–fullerene bulk heterojunction. *Advanced Functional Materials* **15**: 1260–1266.

Schilinsky P, Waldauf C and Brabec CJ (2002) Recombination and loss analysis in polythiophene based bulk heterojunction photodetectors. *Applied Physics Letters* **81**: 3885(1–3).

Shrotriya V, Yao Y, Li G and Yang Y (2006) Effect of self-organization in polymer/fullerene bulk heterojunctions on solar cell performance. *Applied Physics Letters* **89**: 063505(1–3).

Swinnen A and Haeldermans I (2006) Tuning the dimensions of C60 based needlelike crystals in blended thin films. *Advanced Functional Materials* **16**: 760–765.

Tang CW (1986) Two layer organic photovoltaic cell. *Applied Physics Letters* **48**: 183–185.

Wang T, Pearson AJ, Lidzey DG and Jones RAL (2011) Evolution of structure, optoelectronic properties, and device performance of polythiophene:fullerene solar cells during thermal annealing. *Advanced Functional Materials* **21**: 1383–1390.

Yao Y, Hou JH, Xu Z, Li G and Yang Y (2008) Effect of solvent mixture on the nanoscale phase separation in polymer solar cells. *Advanced Functional Materials* **18**: 1783–1789.

Yu G, Gao J, Hummelen JC, Wudl F and Heeger AJ (1995) Polymer photovoltaic cells — enhanced efficiencies via a network of internal donor–acceptor heterojunctions. *Science* **270**: 1789–1791.

Zhang F, Jespersen KG, Björström C *et al.* (2006) Influence of solvent mixing on the morphology and performance of solar cells based on polyfluorene copolymer/fullerene blends. *Advanced Functional Materials* **16**: 667–674.

Zhao Y, Yuan G, Roche P and Leclerc M (1995) A calorimetric study of the phase transitions in poly (3-hexylthiophene). *Polymer* **36**: 2211–2214.

WHAT DO YOU THINK?

To discuss this paper, please email up to 500 words to the managing editor at nme@icepublishing.com

Your contribution will be forwarded to the author(s) for a reply and, if considered appropriate by the editor-in-chief, will be published as a discussion in a future issue of the journal.

ICE Science journals rely entirely on contributions sent in by professionals, academics and students coming from the field of materials science and engineering. Articles should be within 5000-7000 words long (short communications and opinion articles should be within 2000 words long), with adequate illustrations and references. To access our author guidelines and how to submit your paper, please refer to the journal website at www.icevirtuallibrary.com/nme